# Spatially patterned matrix elasticity directs stem cell fate

Chun Yang[a,b], Frank W. DelRio[c], Hao Ma[b,d], Anouk R. Killaars[b,e], Lena P. Basta[d], Kyle A. Kyburz[b,d], and Kristi S. Anseth[b,d,f,1]

[a]Department of Chemistry and Biochemistry, University of Colorado Boulder, Boulder, CO 80303; [b]BioFrontiers Institute, University of Colorado Boulder, Boulder, CO 80303; [c]Material Measurement Laboratory, National Institute of Standards and Technology, Boulder, CO 80305; [d]Department of Chemical and Biological Engineering, University of Colorado Boulder, Boulder, CO 80303; [e]Department of Materials Science and Engineering, University of Colorado Boulder, Boulder, CO 80303; and [f]Howard Hughes Medical Institute, University of Colorado Boulder, Boulder, CO 80303

Contributed by Kristi S. Anseth, June 16, 2016 (sent for review April 11, 2016; reviewed by Andres J. Garcia, Kristopher A. Kilian, and Robert Langer)

**There is a growing appreciation for the functional role of matrix mechanics in regulating stem cell self-renewal and differentiation processes. However, it is largely unknown how subcellular, spatial mechanical variations in the local extracellular environment mediate intracellular signal transduction and direct cell fate. Here, the effect of spatial distribution, magnitude, and organization of subcellular matrix mechanical properties on human mesenchymal stem cell (hMSCs) function was investigated. Exploiting a photodegradation reaction, a hydrogel cell culture substrate was fabricated with regions of spatially varied and distinct mechanical properties, which were subsequently mapped and quantified by atomic force microscopy (AFM). The variations in the underlying matrix mechanics were found to regulate cellular adhesion and transcriptional events. Highly spread, elongated morphologies and higher Yes-associated protein (YAP) activation were observed in hMSCs seeded on hydrogels with higher concentrations of stiff regions in a dose-dependent manner. However, when the spatial organization of the mechanically stiff regions was altered from a regular to randomized pattern, lower levels of YAP activation with smaller and more rounded cell morphologies were induced in hMSCs. We infer from these results that irregular, disorganized variations in matrix mechanics, compared with regular patterns, appear to disrupt actin organization, and lead to different cell fates; this was verified by observations of lower alkaline phosphatase (ALP) activity and higher expression of CD105, a stem cell marker, in hMSCs in random versus regular patterns of mechanical properties. Collectively, this material platform has allowed innovative experiments to elucidate a novel spatial mechanical dosing mechanism that correlates to both the magnitude and organization of spatial stiffness.**

photodegradable hydrogel | human mesenchymal stem cell | spatial matrix stiffness

Tissue homeostasis is maintained by a complex interplay between cells and their surrounding extracellular matrix (ECM), where the ECM is dynamically remodeled and organized on numerous length scales from the subcellular to the macroscopic (1). Although a complex milieu of chemical signals, such as chemokines and cytokines, provide a wealth of cues directing these processes, there is a growing appreciation that contextual presentation of these molecules within the surrounding physical environment can have a dramatic impact on cellular fate as well (2–4). For example, changes in matrix mechanics are important in many biological processes including the recruitment of cells to an injury site during wound healing (5) and during disease development (6, 7). For instance, local ECM organization plays a vital role in breast tumorigenesis, as it is up-regulated by the development of highly cross-linked and linearized local collagen structures, and such abnormal organization can lead to severe tissue stiffening that sustains cancer cell survival and promotes aggressive cellular invasion (8–10). This phenomenon is also observed in heart tissue, where organized ECM is a critical regulator that maintains normal valve function, and disarray of local mechanics provokes pathophysiology such as cardiac hypertrophy or valve calcification (7, 11).

Beyond basic tissue stiffening, matrix spatial organization and the resulting mechanics appear to matter, but how they coordinate a functional stimulus that facilitates intracellular signaling of healthy or diseased phenotypes is poorly understood. Intricate regulation of spatial matrix mechanics is implicated in tissue regeneration during wound healing (12, 13); however, it is challenging to identify individual events of subcellular mechanical stimulation, and investigate how such diverse variations in spatial stiffness integrate to direct local cellular activity. In order to elucidate some of these cell–matrix signaling processes in space, we applied a biomaterial system that allows for the systematic introduction of spatial variations in matrix mechanics. A tunable in vitro platform was developed by exploiting a photolabile chemistry to manipulate material properties of an initially isotropic hydrogel in situ and then examine how spatially patterned elasticity directs the cell fate of human mesenchymal stem cells (hMSCs).

Specifically, we explore whether activating (stiff) and deactivating (soft) mechanical signals, when presented together, obstruct one another, or if there is a threshold at which one signal dominates. To interrogate these hypotheses and their effect on individual stem cell fate, we use a poly(ethylene glycol) (PEG) hydrogel with photolabile linkages that allows for in situ softening of the material modulus on subcellular length scales by controlled light exposure through a photomask. Patterning is achieved on a micrometer scale to create soft (~2 kPa) and stiff (~10 kPa) regions in the hydrogel

## Significance

**The expansion and differentiation of human mesenchymal stem cells (hMSCs), an important cell type that is frequently used in stem-cell–based therapies, are regulated by interactions with their local extracellular microenvironment. Matrix stiffness is one of the key regulators, but often varies in space at a range of length scales in the local niche. To better understand and harness cell–matrix interactions, we used an innovative phototunable hydrogel platform to provide compelling evidence that the magnitude and spatial organization of matrix mechanics influence hMSCs through systematic regulation of cytoskeletal tension and transcriptional activation. These findings may have important implications in deepening our fundamental understanding of the role of extracellular matrix organization on disease, aging, and regenerative processes.**

Author contributions: C.Y., F.W.D., H.M., A.R.K., L.P.B., and K.S.A. designed research; C.Y., F.W.D., H.M., A.R.K., and L.P.B. performed research; C.Y. and F.W.D. contributed new reagents/analytic tools; C.Y., F.W.D., H.M., and A.R.K. analyzed data; and C.Y., F.W.D., K.A.K., and K.S.A. wrote the paper.

Reviewers: A.J.G., Georgia Institute of Technology; K.A.K., University of Illinois at Urbana–Champaign; and R.L., Massachusetts Institute of Technology.

The authors declare no conflict of interest.

Freely available online through the PNAS open access option.

[1]To whom correspondence should be addressed. Email: Kristi.Anseth@colorado.edu.

This article contains supporting information online at www.pnas.org/lookup/suppl/doi:10.1073/pnas.1609731113/-/DCSupplemental.

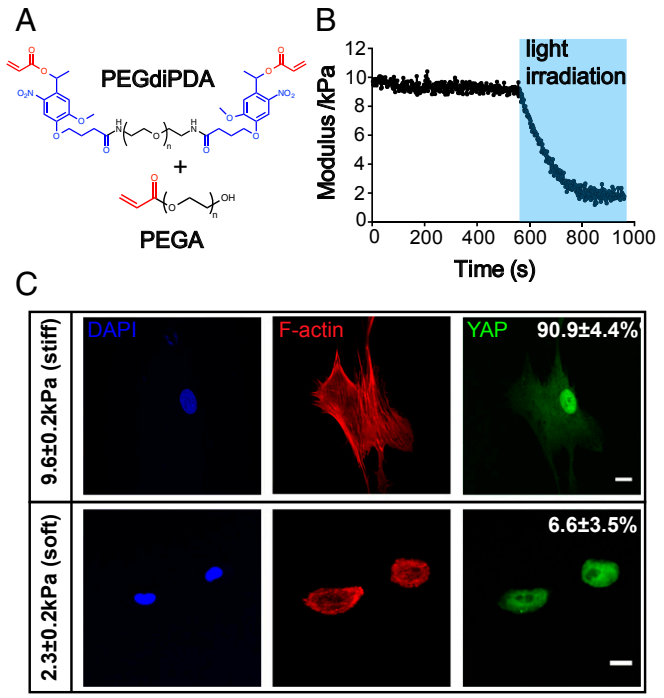


**Fig. 1.** (*A*) Chemical structures of the photodegradable cross-linker (PEGdiPDA) and PEGA. Acrylate functional groups are labeled in red and the photodegradable nitrobenyzl ether is labeled in blue. (*B*) Photodegradable hydrogels polymerized from PEGdiPDA and PEGA monomers can be softened from stiff ($E = 9.6 \pm 0.2$ kPa) to soft ($E = 2.3 \pm 0.2$ kPa) moduli by irradiation of 365 nm light for 360 s. (*C*) Immunostaining of hMSCs on stiff and soft hydrogel surfaces. On stiff hydrogels, hMSCs expressed tensile *F*-actin bundles and had 90.9 ± 4.4% nuclear YAP activation; whereas, on soft hydrogels, hMSCs only had 6.6 ± 3.5% nuclear YAP activation with less organized *F*-actin structure. DAPI (4′,6-diamidino-2-phenylindole; blue) *F*-actin (red), YAP (green). Scale bars = 20 μm; $n = 5$ with over 100 cells analyzed for each condition.

(14). This versatile, user-tunable platform allows one to elucidate how hMSCs respond to mechanical microenvironmental signals that often vary in space, and whether or not cell–matrix interactions lead to mechanotransduction relationships that are linear, step functions, or something more complex.

## Results

Hydrogels with tunable mechanical properties were synthesized by copolymerizing PEG monoacrylate (PEGA) with a photodegradable PEG diacrylate (PEGdiPDA) (Fig. 1*A*). The photolabile cross-linker allows in situ softening of the gel stiffness from an initial Young's modulus ($E$) of 9.6 ± 0.2 kPa to 2.3 ± 0.2 kPa by exposure to 365 nm light at 10 mW/cm$^2$ for 360 s (Fig. 1*B*). Cytoskeletal organization of hMSCs seeded on the hydrogel formulation with the highest modulus (subsequently referred to as stiff, $E = 9.6 \pm 0.2$ kPa) exhibited more organized actin bundles, as indicated by *F*-actin staining, and tensile actomyosin fibers compared with those cultured on gel with the lowest modulus (subsequently referred to as soft; $E = 2.3 \pm 0.2$ kPa) (Fig. 1*C*, *Middle*). In addition, seeding on uniformly stiff substrates led to 90.9 ± 4.4% nuclear Yes-associated protein (YAP) (15) activation, although YAP was mostly deactivated in the cytoplasm with only 6.6 ± 3.5% nuclear localization for hMSCs cultured on the softer gel (Fig. 1*C*, *Right*), indicating that two opposite intracellular signals are induced in this range of matrix mechanical properties.

Subsequently, the aforementioned stiff and soft signals were introduced to hMSCs on the same surface through controlled softening of the hydrogel via spatial degradation of the nitrobenzyl ether cross-linker by passing light through a photomask and examining how spatial variations in mechanical signaling influences hMSC response. We aimed to pattern mechanical regions that were comparable in size to a mature focal adhesion (1 to 5 μm$^2$) (16, 17); so that spatial mechanical variations would be introduced at a length scale that can potentially direct focal adhesion assembly and subsequently affect cellular attachment and internal mechanotransduction. Uniform patterns of 2 μm by 2 μm squares were created to introduce regions with distinct mechanical properties; specifically, after light exposure, the ratio of stiff to soft regions was varied as indicated in Fig. 2*A*. Also, because the average area of a spread hMSC is ~1,500 μm$^2$ on uniformly soft substrates (Fig. S1), the cells should sample a large number of both stiff and soft regions. Thus, statistically, any single hMSC on the substrate should experience a similar composition of mechanical cues.

Using several different lithographic masks, cell culture substrates were synthesized with varying patterns to study the effects of a range of different stiff to soft ratios (3:1, 1:1, 1:3, 1:8) and corresponding areas of stiffness (75%, 50%, 25%, and 11%, respectively) on hMSC matrix interactions and signaling. The resulting patterned substrates were characterized by atomic force microscopy (AFM) as shown in Fig. 2*B*; representative images for the regular 75% and 11% stiff, as well as random 75% stiff substrates are shown in Figs. 2*B*, i, ii, and iii, respectively. As evident from the AFM data, the spatial variations in the moduli values are consistent with the patterns found on the lithographic masks, indicating successful pattern transfer to the intended regions of the hydrogels using photosoftening. In addition,

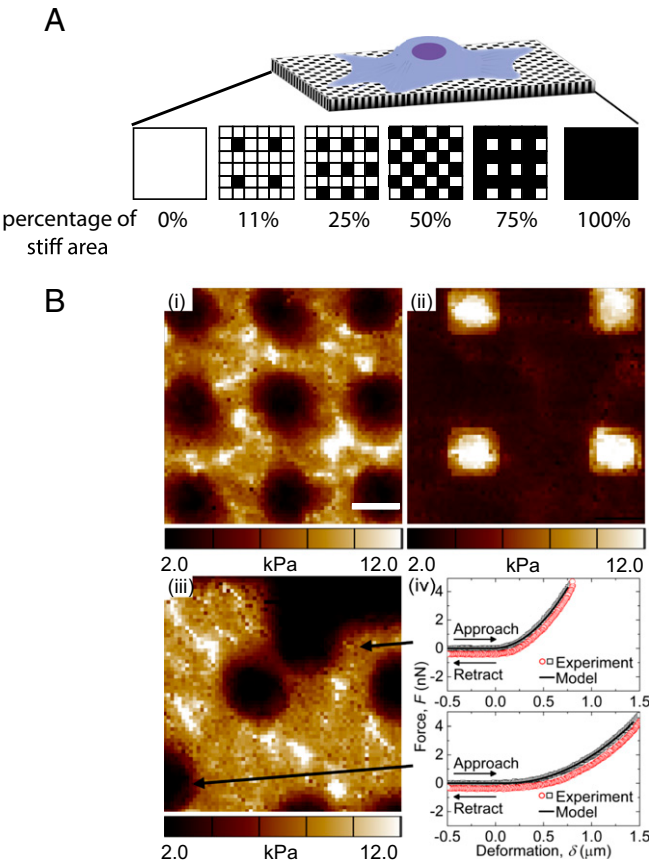


**Fig. 2.** (*A*) An illustration of hMSCs seeded on mechanically patterned hydrogel surfaces with different stiff-to-soft ratios. Black indicates chrome-covered areas that will remain stiff, and white squares indicate areas exposed to light that will be degraded to soft regions. (*B*) AFM elastic moduli maps of (*i*) 75% stiff (regular pattern), (*ii*) 11% stiff (regular pattern), and (*iii*) 75% stiff (random pattern) hydrogels. (*iv*) Representative force-deformation data and model fits for two regions in *iii*. Scale bars = 2 μm.

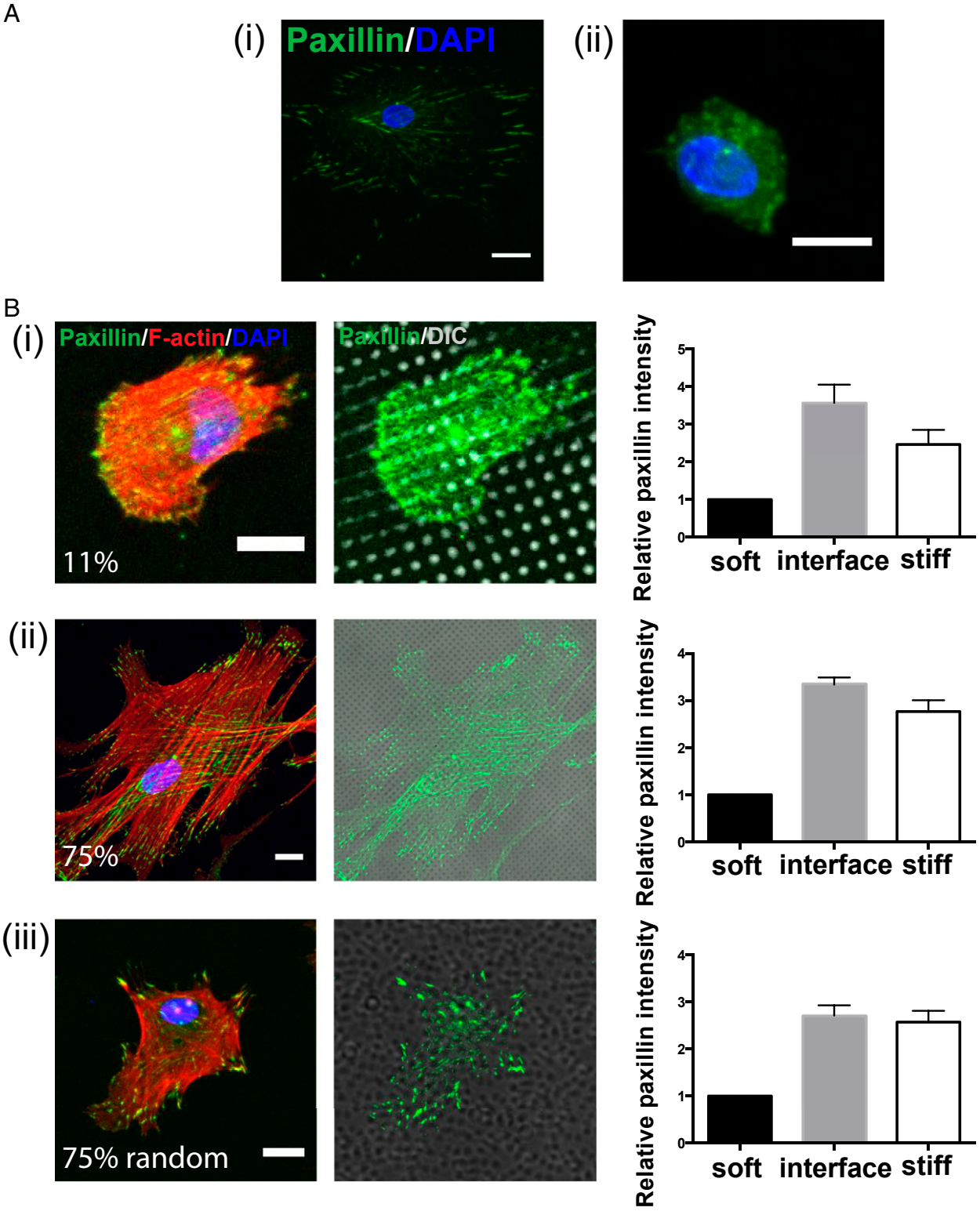


**Fig. 3.** (*A, i*) Paxillin staining (green) of hMSCs on stiff hydrogels illustrates clustered structures, which indicate the formation of mature focal adhesion. (*ii*) However, paxillin staining of hMSCs seeded on soft hydrogels results in a basal uniform expression throughout the cell body. Paxillin (green); DAPI (blue). Scale bars = 20 μm. (*B*) Relative localization of focal adhesions in hMSCs to mechanical regions on the patterned hydrogel. (*i*) Immunostaining of hMSCs on a regularly patterned hydrogel with 11% stiff area. Focal adhesion formation was observed by staining for paxillin (green), and cytoskeletal organization was observed by staining for *F*-actin (red). The localization of focal adhesions relative to the mechanically patterned regions was analyzed to identify the relative paxillin intensity within stiff, soft, and interfacial regions based on the fluorescent and DIC channels (*Right*). For quantification, all paxillin intensities for each image were normalized to the absolute value found in the soft regions. (*ii*) Immunostaining of hMSCs on regularly patterned hydrogel with 75% stiff area. (*iii*) Immunostaining of hMSCs on randomized patterned hydrogel with 75% stiff area. In all three conditions, paxillin intensities were about threefold higher in the stiff and interfacial regions relative to the soft regions. Paxillin (green), *F*-actin (red), DAPI (blue). Scale bars = 20 μm; $n > 10$ with over 50 cells analyzed for each condition. Data plotted as mean ±SE.

the magnitude of the moduli measured using AFM are in good agreement with rheological bulk moduli measurements (Fig. 1*B*, Fig. S2) of the uniformly stiff and soft substrates, with values ranging from ∼2–3 kPa in the soft regions to ∼10–12 kPa in the stiff regions. For reference, two AFM force (*F*)–deformation (δ) datasets from Fig. 2*B*, *iii* are shown in Fig. 2*B*, *iv*. In both the soft and stiff regions, the AFM *F*–δ data are well-described by the model used to extract the moduli values (i.e., *F* is proportional to $\delta^2$), suggesting that the contact geometry between the AFM tip and hydrogel surface is well approximated by the analytical solution for a rigid conical indenter in contact with an elastic half-space.

Complementary to the mechanical property measurements, the surface roughness after gel patterning was also analyzed by AFM, as surface topography has been shown to influence cell fate (18, 19). After photopatterning, the hydrogel surface (75% stiff) had an rms roughness of 43 ± 2 nm, which is on the same order of magnitude compared with the rms roughness of 12 ± 1 nm on the uniformly stiff hydrogel, and 23 ± 2 nm on the uniformly soft hydrogel (Fig. S3). Therefore, hydrogels were fabricated with distinctly varying mechanical regions with minimal changes in the surface topography that maintain a constant adhesive area among conditions of different stiff-to-soft ratios.

Subsequently, markers of cell–matrix interactions were examined to determine whether hMSCs can distinguish between differences in mechanical properties on the μm scale, or if they simply sense the overall average stiffness. Both the *F*-actin structure and the focal adhesion protein paxillin were stained for hMSCs cultured on surfaces with spatially varying mechanical moduli (Fig. 3). In general, punctate paxillin staining, indicating mature focal adhesions (20), was observed at the cell–matrix interface when hMSCs were cultured on the uniformly stiff substrates (Fig. 3*A*, *i*). In contrast, hMSCs on the soft substrate (Fig. 3*A*, *ii*) had uniform basal paxillin expression throughout the cell body instead of forming clustered structures at the interface, indicating that fewer mature focal adhesions were formed. It is interesting to note that when hMSCs were cultured on patterned surfaces, punctate paxillin staining appeared to concentrate in the stiff regions and along the border of stiff-to-soft regions. This observation was further quantified by using image analysis that first identified stiff and soft regions of the hydrogel surface based on bright field images [differential interference contrast (DIC channel)] and then calculated the relative focal adhesion intensity (normalized to area) in both regions with mechanically distinct properties, as well as within an interfacial edge between them (Fig. 3*B*; Fig. S4). For hMSCs on both 11% (Fig. 3*B*, *i*) and 75% (Fig. 3*B*, *ii*) stiff substrates, the focal adhesion intensities within the interfacial region and stiff regions were almost threefold higher, compared with that measured in the soft regions. However, with distinct clustered paxillin structures, many more tensile *F*-actin fibers were observed to initiate from focal adhesion sites in the stiff regions when hMSCs were on 75% stiff substrates than those cultured on 11% stiff substrates. This observation implies that cytoskeletal tension in hMSCs, which is much stronger on substrates with a higher fraction of stiff regions, is generated as a function of the mechanical property patterning (Fig. 3*B*, *i* and *ii*).

In addition, we hypothesized that the spatial organization of the stiff versus soft regions, which plays an important role in the regulation of actin structure formation in hMSCs, would also affect cell–matrix signal transduction. Therefore, we created materials with the same ratio of soft and stiff regions, but distributed the regions in a random (or disorganized) manner as shown in Fig. S5 and validated in Fig. 2*B*, *iii* to investigate the corresponding cell responses. Specifically, hydrogels were fabricated by a repeating 50 μm by 50 μm (2,500 $\mu m^2$) square pattern, in which the locations of the 2 μm by 2 μm stiff and soft regions were randomized. This patterned region is on the same size scale as a spread hMSC (Fig. S1), so the repeat unit is large enough for a single cell to sense these variations. When hMSCs were cultured on the random 75% stiff substrate (Fig. 3*B*, *iii*), punctate paxillin was again observed to colocalize with the stiff regions and with a similar distribution on stiff, soft, and interfacial regions as that found on the regular patterns (Fig. 3*B*, *iii*, *Right*). *F*-actin fibers stemmed from these focal adhesion sites; however, due to the differences in spatial organization of the focal adhesions, hMSCs on the random patterns had less organized tensile actin bundles than those on the regular pattern, even on hydrogels with the same percentage of stiff regions.

Based on the differences observed in hMSC–matrix interactions on substrates with varying percentages of stiff and soft regions and between regular and random patterns, we next sought to investigate whether or not these differences in cytoskeletal tension would lead to activation of the subcellular transcriptional coactivator YAP, the mediator that gauges extracellular mechanical stimulations into genetic events that can eventually affect hMSCs differentiation (15, 21, 22). Specifically, when hMSCs sense competing mechanical signals, does a threshold or critical interfacial area exist that a cell needs to sense in order for it to accumulate sufficient cytoskeletal tension to sustain nuclear YAP activation? Moreover, how will the spatial organization of mechanical signals play a role in such regulation? To answer these questions, hMSCs were studied on substrates patterned with regular 11% and 75% stiff regions, which represent two distinct stiff and soft ratios regimes from the cytoskeleton tension analysis (Fig. 4*A*, *i* and *ii*). Intracellular YAP localization was visualized by immunostaining, and more prominent nuclear YAP localization was observed on the substrate with 75% stiff moduli; however on 11% stiff substrates, YAP mainly remained inactive and localized in the cytoplasm (Fig. 4*A*, *i* and *ii*). This activation level was quantified based on the percentage of cells that had nuclear YAP staining, which was 83.4 ± 6.9% and 11.6 ±4.5%, respectively (Fig. 4*B*, *i*).

Based on this analysis, further investigations were performed to study whether there was a functional relationship that might dictate intracellular YAP activation in hMSCs when they experience these variations in spatial stiffness. To this end, hMSCs were seeded on hydrogels with regularly patterned 0%, 11%, 25%, 50%, 75%, and 100% stiff regions as shown in Fig. 2*A*. A sigmoidal response was observed (Fig. 4*B*, *i*), in which less than 20% activation was observed on surfaces with 0%, 11%, and 25% stiff regions; whereas, a statistically significant higher level of YAP activation was induced when the underlying substrates were increased from 25% to 50% stiffness, but the trend plateaus near 75% stiffness.

Because of the differences in cellular attachment and cell–matrix interactions on regular and randomly patterned surfaces (Fig. 3*B*), an additional investigation was performed to characterize YAP localization when hMSCs were seeded onto substrates with randomized stiffness regions. To our surprise, when hMSCs were cultured on the 75% random stiff pattern, YAP was mostly deactivated in the cytoplasm with only 35.4 ± 6.5% nuclear localization (Fig. 4 *A, iii,* and *B, i*), which was significantly lower than the 83.4 ± 6.9% intracellular YAP activation in hMSCs on 75% stiff regular patterns. Additional random patterns were generated from 11% to 75% spatial stiffness; however, no statistically significant elevation in YAP activation was observed as the spatial stiffness increased, in contrast to the cellular response on the gels with regularly distributed stiffness (Fig. 4*B, i*). These results implied to us that a mechanism other than a dose response may be regulating the mechanotransduction process when the spatial organization of the matrix stiffness is disrupted. These differences were further quantified by comparing gene expression levels of ANKRD1 and CTGF, two of the genes that are up-regulated by the activity of YAP (15). Results show that there is significantly higher expression of both ANKRD1 and CTGF for hMSCs cultured on regularly spaced 75% stiff patterns compared with 75% randomized stiff patterns (Fig. 4*B, ii*).

Complementary to these experiments, it was then investigated whether cell morphology correlated with the activation trend observed with the mechanosensor YAP in response to spatial mechanical dosing for both the regular and random patterns. On uniformly stiff substrates, hMSCs spread to an area of 4,290 ± 163 $\mu m^2$, which is approximately a threefold increase relative to

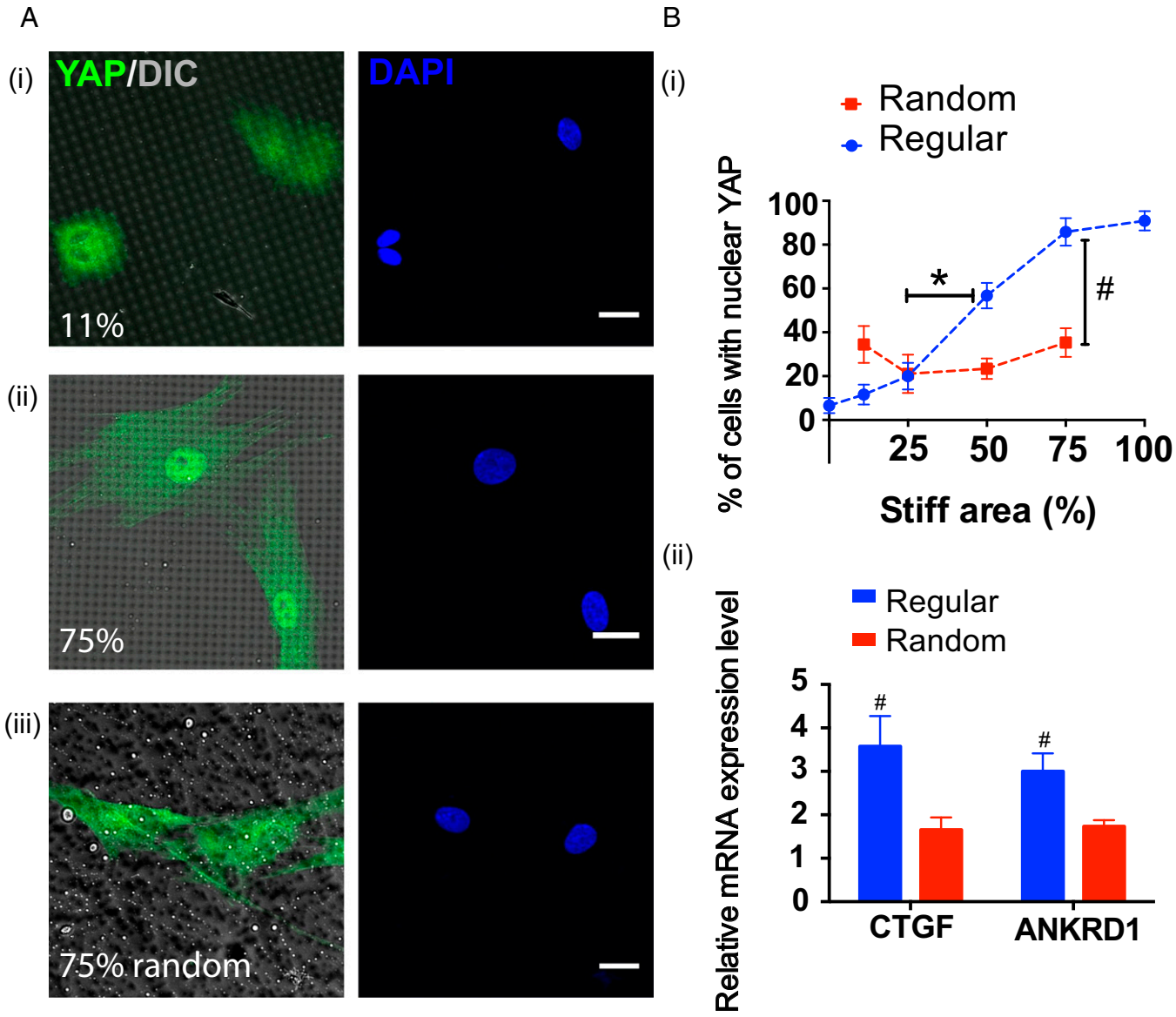


**Fig. 4.** (*A, i*) Intracellular YAP (green) localization within hMSCs on regularly patterned hydrogels with 11% stiff area. Image was overlaid with the DIC channel to indicate the underlying pattern. YAP was mainly deactivated in the cytoplasm on 11% stiff hydrogels. (*ii*) Intracellular YAP localization of hMSCs on regularly patterned hydrogels with 75% stiff area. YAP was observed to primarily be activated in the nuclei. (*iii*) Intracellular YAP localization of hMSCs on randomly patterned hydrogels with 75% stiff area. YAP was found to be mainly deactivated in the cytoplasm. YAP (green), DAPI (blue). Scale bars = 20 μm. (*B, i*) The percent of hMSCs with intracellular YAP activation was quantified based on immunostaining analysis and found to increase correspondingly to stiff percentages on regular stiff patterns, indicated by the blue dash line and symbols. A sigmoidal response was observed with a significant increase in YAP activation from 25% stiff to 50% stiff. However, on randomly patterned hydrogels intracellular YAP activation in hMSCs was insensitive to the change of underlying stiff percentages, indicated by the red dash line and symbols; $n > 5$ with over 100 cells analyzed for each condition; * compared with regular 25% stiff, $P < 0.01$ based on one-way ANOVA analysis using Turkey's multiple comparisons test; # compared with random 75% stiff, $P < 0.001$ based on unpaired $t$ test. (*ii*) Comparison of relative mRNA expression levels of the genes CTGF and ANKRD1 for hMSCs on regularly and randomly patterned hydrogels with 75% stiff regions. For both genes, hMSCs on regular patterns had significantly higher expression levels than those on the random patterns. $n = 3$. # $P < 0.05$, based on unpaired $t$ test.

those on uniformly soft microenvironments (1,431 ± 84 μm$^2$) (Fig. 5*A*). Previous reports have noted that YAP activation can be regulated by cell geometry through differences in cytoskeletal tension (15). When cultured on hydrogels with regularly spaced patterns of mechanical properties, the hMSC area was observed to increase in a manner that corresponded to the percentage of stiff regions, and a dramatic increase in cell area (2,338 ± 173 μm$^2$ to 4,429 ± 757 μm$^2$) was observed when the hydrogel mechanics increased from 50% to 75% stiff (Fig. 5*A*, blue dashed line and symbols). In contrast, cell spreading remained around 2,400 μm$^2$ on hydrogels with random patterns: from 2,430 ± 265 μm$^2$ on the 11% stiff to 2,483 ± 221 μm$^2$ on the 75% stiff samples regardless of the stiff to soft ratio (Fig. 5*A*, red dashed line and symbols). Beyond measurements of cell spreading, circularity was also examined, as it can be a quantitative indicator of cytoskeletal tension (23) (Fig. 5*B*). Consistent with other measurements, circularity of hMSCs decreased correspondingly to the spatial stiffness area on the regular patterned surfaces (Fig. 5*B*, blue dashed line and symbols); but was insensitive to increases in stiff regions on the randomly patterned gels (Fig. 5*B*, red dashed line and symbols).

The presented data suggest that the magnitude and spatial organization of a cell's mechanical matrix environment are coupled and

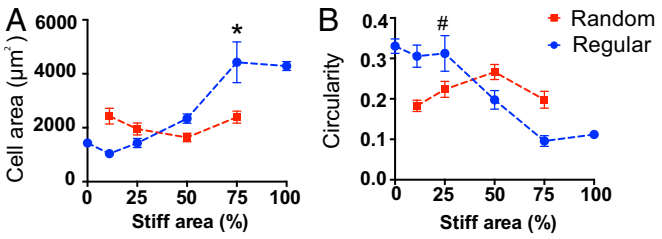


**Fig. 5.** (*A*) Cell spreading area increased correspondingly to stiff percentages on regularly patterned hydrogels, indicated by the blue dashed line and symbols, consistent with the trend of intracellular YAP activation. A significant increase of cell area was observed from 50% to 75% stiff gels. On the other hand, cell spreading was insensitive to the change of underlying stiff percentages on randomly patterned hydrogels, indicated by the red dashed line and symbols; * compared with regular 50% stiff, $P < 0.01$ based on one-way ANOVA using Tukey's multiple comparisons test. (*B*) Complimentary, cellular circularity decreased relative to stiff percentages on regularly patterned hydrogels, indicated by the blue dashed line and symbols. However, circularity did not change significantly with increased stiff area on randomly patterned hydrogels, indicated by the red dash line and symbols; # compared with 75% regular stiff, $P < 0.01$ based on one-way ANOVA; $n > 5$ with over 100 cells analyzed for each condition. Mean ± SE.

converge to be a functional regulator of hMSCs by influencing their morphology and activating internal mechanotransduction sensors. Based on this supposition, we hypothesized that the effect of regular and random patterns of matrix mechanics in a cell's niche can lead to divergence in hMSC fate. To this end, we investigated hMSC osteognesis by culturing them on regularly and randomly patterned hydrogels with 75% stiff regions. First, alkaline phosphatase (ALP) staining was performed (Fig. 6*A*), and cells on the regularly patterned gels were more spread, larger in area, and stained darker, indicating a higher expression of the osteogenic marker ALP, and found to be similar to hMSCs cultured on the uniformly stiff gels. In contrast, minimal staining was observed in hMSCs cultured on randomly patterned surfaces and uniformly soft surfaces, suggesting a significantly lower level of osteogenesis (Fig. 6*A*). It is intriguing to note that a significantly higher level of expression of the stem cell marker CD105 was observed in hMSCs that were cultured on either the random patterned gels or the uniformly soft hydrogels (Fig. 6*B*), implying that the randomized stiff cues were arranged in a manner that inhibit hMSCs osteogenesis.

## Discussion

Previous investigations of subcellular adhesive ligand organization (17, 24–26) and surface nanotopography features (18, 19, 27) on stem cell behavior demonstrated the fundamental role of ECM structure in directing cell–matrix interactions. However, the effect of matrix mechanics is still largely unknown. Specifically, it is challenging to precisely define and elucidate the spatial organization and presentation of matrix mechanics in vivo and in cellular culture platforms. For example, the heterogeneous chemical composition of native bone tissue leads to varied mechanical properties on a wide range of length scales. This homeostasis is disrupted by physical deformity upon injury and subsequent inflammatory response, leading to disorganized chemical and physical structures in the local cell microenvironment (28). Other examples in liver pathology further emphasize the regulatory role of matrix organization in fibrotic diseases through the modulation of tissue morphogenesis, in which the functional hepatic architecture is disturbed by an abnormal accumulation of ECM proteins and lead to fibrous scar and subsequent cirrhosis (29–33). Elucidating how cells, especially stem cells that are recruited to the wound site, distinguish and respond to these discrepancies in the mechanical environment is critical for the field to deepen our collective understanding of the tissue regeneration process. Here, we applied a unique phototunable hydrogel system to introduce and characterize the effects of spatial variations in mechanical properties on cells cultured on the matrices. We observed that spatially altering mechanical stiffness affects hMSCs in a dose-dependent manner through the regulation of cytoskeletal tension and intracellular transcriptional activation. Specifically, focal adhesion formation colocalized with activating, stiff regions on hydrogel substrates, which in turn directed the formation of the actin cytoskeleton structure. Increasing the stiffness ratio on regularly patterned hydrogels promoted YAP activation, as well as increased cell spreading and led to more elongated cell morphologies. It is interesting to note that hMSCs became insensitive to increases in the spatial stiffness of their microenvironment if the regions were arranged in a randomized manner. Further, the randomization was observed to disrupt the actin structure, reduce YAP activation, and decrease cell spreading.

This dosing response was found to be specific to the presentation of spatially patterned mechanical regions, but independent of similar spatial variations in adhesive area among the different patterns. As previously reported, 95% of the adhesive ligand RGD remains attached after cleavage of the cross-linker because it was conjugated to the nondegradable region of the network (21), so that the mechanically patterned hydrogel has a relatively homogenous adhesive ligand concentration across stiff and soft regions. Additional experiments were conducted to ensure that the ∼5% decrease in RGD concentration in the soft area after irradiation did not affect cellular morphology and downstream transcriptional activation events (Fig. S6). As another control experiment, we introduced the adhesive protein fibronectin onto hydrogels of a uniform modulus of elasticity, in this case the stiffer formulation, and then created patterns of adhesive and nonadhesive areas (24). In this system, no significant differences in YAP activation (∼90%; Fig. S7) were observed in hMSCs when they were exposed to adhesive ligands that were regularly patterned in 25%, 87%, or randomly patterned in 25% of the area. These results further support the conclusion that the observed trend in YAP activation is not regulated through variations in ECM contact area, but is defined by spatial variations in mechanical signals that induce different magnitudes of cytoskeletal tension.

Previous literature has indicated that surface roughness is a potent physical cue that affects cell–ECM interactions (27, 34, 35). As we aimed to define and independently vary spatial stiffness, we

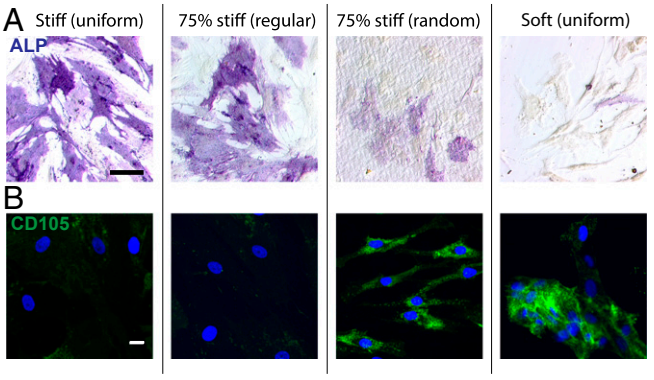


**Fig. 6.** (*A*) ALP staining of hMSCs on uniformly stiff, 75% stiff with regular and random patterns and uniformly soft hydrogels after 7 d culture in mixed media. hMSCs on uniformly stiff and regularly patterned 75% stiff samples had prominent ALP expression; but the expression levels were significantly lower on the randomly patterned 75% stiff and uniformly soft samples. ALP (purple). Scale bar = 100 μm. (*B*) CD105 staining of hMSCs on uniformly stiff, 75% stiff with regular and random patterns and uniformly soft hydrogels after 7 d culture in mixed media. hMSCs on uniformly soft and randomly patterned 75% stiff samples had significantly higher CD105 expressions than those on uniformly stiff and regularly patterned 75% stiff samples. CD105 (green), DAPI (blue). $n = 3$. Scale bar = 20 μm.

carefully designed and optimized the photodegradation procedure to minimize significant differences in surface topography. In multiple examples, significant changes in cellular behavior and stem cell markers have been observed when MSCs sense topographical features > 100 nm, e.g., between $R_q$ 1 and 100 nm (35); on 100-nm topography features (19) and on 300-nm topography features (34). Therefore, we expected the effect of rms roughness (43 ± 2 nm) on hMSC responses to patterned surfaces to be minimized, because the compliant and flexible nature of the hydrogel rendered systems with minimal changes in nanoscale topography feature that would significantly alter cellular attachment and cytoskeletal structure.

Finally, osteogenic differentiation of hMSCs cultured on hydrogels with regularly patterned mechanical regions was significantly higher than those cultured on random patterns, as measured by ALP staining. Complementary, the randomized stiffness patterns promoted a higher CD105 expression in hMSCs, thus demonstrating the regulatory role of the spatial organization of the local environmental stiffness in determining cell fate decisions. Collectively, these observations support the notion that mechanical dosing influences hMSCs, but in a manner that correlates to both spatial distribution and organization of the matrix mechanics.

In previous work by Dalby et al. (19), it was reported that nanotopography features that were randomly introduced on poly (methyl methacrylate) surfaces promoted cell adhesion (long fibrillarlike adhesions) and subsequent higher osteogenic differentiation than surfaces with more orderly and organized nanotopography features. Although we are using two quite different platforms, e.g., rigid poly (methyl methacrylate) surfaces vs. compliant hydrogel substrates; nanoscale topography vs. micrometer-scale mechanical patterns, our findings support similar conclusions, which are: organization of extracellular matrix impacts stem cell signaling through systematic regulation of cytoskeletal structure, transcriptional activation, and gene expression profile. In our study, we observed that the regularly spaced micrometer-scale mechanical pattern promoted a focal adhesion structure that induced higher cytoskeletal tension (Fig. S8), which further led to YAP activation and enhanced osteogenesis. On the other hand, Dalby et al. observed that certain disordered nanotopographical features alter cellular cytoskeletal structure in a way that lead to distinct gene expression profiles, which promote osteogenesis. It is clear that the morphological changes in cytoskeletal structure upon cell–ECM interaction initiates the downstream transduction of extracellular signal, which implies that a complex interplay between integrin expression, surface chemistry, protein conformation, topography, and mechanics most likely intersect to influence the overall cell–ECM contact.

Taken as a whole, our results begin to provide insight into stem cell behavior during dynamic events that occur during matrix remodeling, as to whether the organization of the matrix environment acts as a mechanical "switch" for cell lineage decisions. These findings highlight the importance of new biomaterial matrices that allow experimenters intimate control of cell-matrix interactions and signaling. Innovations in biomaterial chemistry are enabling novel experiments to be performed that are improving the field's understanding of mechanotransduction, especially as it relates to changes in cell behavior that occurs during tissue remodeling in development, disease processes, and wound healing.

## Materials and Methods

Human mesenchymcal stem cells (hMSCs) were isolated from fresh human bone marrow (Lonza). P2 hMSCs were used in these experiments. Distinct mechanical regions were introduced on the photodegradable hydrogels by photopatterning using 36 nm light and characterized by AFM. Cellular morphology, gene expressions, and differentiations on the patterned substrates were analyzed similar to previous studies (21). For complete details of materials and methods, please refer to *Supporting Information*.

**ACKNOWLEDGMENTS.** We thank Eric Bunker for developing the Matlab code for image analysis, Dr. Joseph Grim for manuscript editing, and Prof. Virginia Ferguson and Dr. Emi Tokuda for helpful discussions on the work, as well as Dr. Joe Dragavon for assistance in image acquisition. This work was supported by the National Institutes of Health (Grants R01 DE016523 and R21 AR067469) and the Howard Hughes Medical Institute (K.S.A.).

1. Engler AJ, Humbert PO, Wehrle-Haller B, Weaver VM (2009) Multiscale modeling of form and function. *Science* 324(5924):208–212.
2. Engler AJ, Sen S, Sweeney HL, Discher DE (2006) Matrix elasticity directs stem cell lineage specification. *Cell* 126(4):677–689.
3. Lutolf MP, Gilbert PM, Blau HM (2009) Designing materials to direct stem-cell fate. *Nature* 462(7272):433–441.
4. Gilbert PM, et al. (2010) Substrate elasticity regulates skeletal muscle stem cell self-renewal in culture. *Science* 329(5995):1078–1081.
5. Morrison SJ, Spradling AC (2008) Stem cells and niches: Mechanisms that promote stem cell maintenance throughout life. *Cell* 132(4):598–611.
6. Bonnans C, Chou J, Werb Z (2014) Remodelling the extracellular matrix in development and disease. *Nat Rev Mol Cell Biol* 15(12):786–801.
7. Hinton RB, Yutzey KE (2011) Heart valve structure and function in development and disease. *Annu Rev Physiol* 73:29–46.
8. Egeblad M, Rasch MG, Weaver VM (2010) Dynamic interplay between the collagen scaffold and tumor evolution. *Curr Opin Cell Biol* 22(5):697–706.
9. Levental KR, et al. (2009) Matrix crosslinking forces tumor progression by enhancing integrin signaling. *Cell* 139(5):891–906.
10. Provenzano PP, et al. (2006) Collagen reorganization at the tumor-stromal interface facilitates local invasion. *BMC Med* 4(1):38.
11. Schoen FJ (2008) Evolving concepts of cardiac valve dynamics: The continuum of development, functional structure, pathobiology, and tissue engineering. *Circulation* 118(18):1864–1880.
12. Augat P, Simon U, Liedert A, Claes L (2005) Mechanics and mechano-biology of fracture healing in normal and osteoporotic bone. *Osteoporos Int* 16(Suppl 2):S36–S43.
13. Klein P, et al. (2003) The initial phase of fracture healing is specifically sensitive to mechanical conditions. *J Orthop Res* 21(4):662–669.
14. Kloxin AM, Kasko AM, Salinas CN, Anseth KS (2009) Photodegradable hydrogels for dynamic tuning of physical and chemical properties. *Science* 324(5923):59–63.
15. Dupont S, et al. (2011) Role of YAP/TAZ in mechanotransduction. *Nature* 474(7350):179–183.
16. Scales TME, Parsons M (2011) Spatial and temporal regulation of integrin signalling during cell migration. *Curr Opin Cell Biol* 23(5):562–568.
17. Chen CS (1997) Geometric control of cell life and death. *Science* 276(5317):1425–1428.
18. McMurray RJ, et al. (2011) Nanoscale surfaces for the long-term maintenance of mesenchymal stem cell phenotype and multipotency. *Nat Mater* 10(8):637–644.
19. Dalby MJ, et al. (2007) The control of human mesenchymal cell differentiation using nanoscale symmetry and disorder. *Nat Mater* 6(12):997–1003.
20. Turner CE (2000) Paxillin and focal adhesion signalling. *Nat Cell Biol* 2(12):E231–E236.
21. Yang C, Tibbitt MW, Basta L, Anseth KS (2014) Mechanical memory and dosing influence stem cell fate. *Nat Mater* 13(6):645–652.
22. Halder G, Dupont S, Piccolo S (2012) Transduction of mechanical and cytoskeletal cues by YAP and TAZ. *Nat Rev Mol Cell Biol* 13(9):591–600.
23. McBeath R, Pirone DM, Nelson CM, Bhadriraju K, Chen CS (2004) Cell shape, cytoskeletal tension, and RhoA regulate stem cell lineage commitment. *Dev Cell* 6(4):483–495.
24. Trappmann B, et al. (2012) Extracellular-matrix tethering regulates stem-cell fate. *Nat Mater* 11(7):642–649.
25. Lee TT, et al. (2015) Light-triggered in vivo activation of adhesive peptides regulates cell adhesion, inflammation and vascularization of biomaterials. *Nat Mater* 14(3):352–360.
26. Petrie TA, et al. (2010) Multivalent integrin-specific ligands enhance tissue healing and biomaterial integration. *Sci Transl Med* 2(45):45ra60.
27. Dalby MJ, Gadegaard N, Oreffo ROC (2014) Harnessing nanotopography and integrin-matrix interactions to influence stem cell fate. *Nat Mater* 13(6):558–569.
28. Rho J-Y, Kuhn-Spearing L, Zioupos P (1998) Mechanical properties and the hierarchical structure of bone. *Med Eng Phys* 20(2):92–102.
29. Bataller R, Brenner DA (2005) Liver fibrosis. *J Clin Invest* 115(2):209–218.
30. Ingber DE (2002) Cancer as a disease of epithelial-mesenchymal interactions and extracellular matrix regulation. *Differentiation* 70(9-10):547–560.
31. Bosman FT, Stamenkovic I (2003) Functional structure and composition of the extracellular matrix. *J Pathol* 200(4):423–428.
32. Ingber DE (2003) Mechanobiology and diseases of mechanotransduction. *Ann Med* 35(8):564–577.
33. Cox TR, Erler JT (2011) Remodeling and homeostasis of the extracellular matrix: implications for fibrotic diseases and cancer. *Dis Model Mech* 4(2):165–178.
34. Pan F, et al. (2013) Topographic effect on human induced pluripotent stem cells differentiation towards neuronal lineage. *Biomaterials* 34(33):8131–8139.
35. Chen W, et al. (2012) Nanotopography influences adhesion, spreading, and self-renewal of human embryonic stem cells. *ACS Nano* 6(5):4094–4103.
36. Kloxin AM, Tibbitt MW, Anseth KS (2010) Synthesis of photodegradable hydrogels as dynamically tunable cell culture platforms. *Nat Protoc* 5(12):1867–1887.
37. Hutter JL, Bechhoefer J (1993) Calibration of atomic-force microscope tips. *Rev Sci Instrum* 64(7):1868–1873.
38. Sneddon IN (1965) The relation between load and penetration in the axisymmetric boussinesq problem for a punch of arbitrary profile. *Int J Eng Sci* 3(1):47–57.
39. Mariner PD, Johannesen E, Anseth KS (2012) Manipulation of miRNA activity accelerates osteogenic differentiation of hMSCs in engineered 3D scaffolds. *J Tissue Eng Regen Med* 6(4):314–324.